Staging of gastrulating mouse embryos by morphological landmarks in the dissecting microscope

Karen M. Downs* and Tim Davies

Imperial Cancer Research Fund, Developmental Biology Unit, Department of Zoology, University of Oxford, South Parks Road, Oxford OX1 3PS, UK

*Author for correspondence

SUMMARY

We describe and illustrate a set of morphological landmarks for classifying mouse embryos by gross morphology from before gastrulation to the beginning of organogenesis. These landmarks are visible at the resolution of the dissecting microscope in embryos that are intact except for reflexion of Reichert's membrane.

Adoption of these criteria should facilitate interpretation of both the expression patterns of genes and the consequences of experimental manipulation of embryos during early postimplantation development.

Key words: gastrulation, staging, mouse

INTRODUCTION

Gastrulation is the period in postimplantation development when a single-layered epithelium, called the primitive ectoderm, is transformed progressively into three tissue layers, and acquires simultaneously the axial organization characteristic of the future fetus. It begins at about 6.75 days postcoitum, some time after implantation and, over the next 48 hours, the three primary germ layers are established and interact in coordinated fashion to form the primordia of fetal organs.

Recent interest in mammalian gastrulation has been fuelled by the recognition that certain families of growth factors and their receptors may participate in mesoderm induction in amphibians. Unlike the gastrulating frog embryo, the gastrulating mouse embryo is inaccessible to manipulation within the implantation site, but recent technical advances of whole-embryo culture now enable the entire period of gastrulation to be studied from its onset (Lawson et al., 1991). Most of the current work on mouse gastrulation involves the localization of transcripts of potentially important developmental genes, such as growth factors and proto-oncogenes, by hybridization in situ to cells and tissues of the gastrulating mouse embryo. With the gap between classical embryology and molecular genetics bridged, the only major impediment to reproducibility between studies and comparability within studies is the lack of a common stage system during mouse gastrulation.

With few exceptions, mouse embryologists generally rely upon 'days postcoitum' ('dpc') to stage gastrulating mouse embryos (Rugh, 1968; Theiler, 1989; Snell and Stevens, 1966; Kaufman, 1991; 1992). However, their staging method is difficult to generalize between studies due to variations in (a) the rate of development of mouse strains, (b) differences in lighting regimes under which mice are bred and (c) variation between littermates in a single litter. These sources of inaccuracy complicate the comparison of gene expression studies during mouse gastrulation, when only 'days postcoitum' are reported, and makes difficult the compilation of precise timing and location of expressed genes, especially those expressed transiently during the first 72 hours of gastrulation (see, for example, Blum et al., 1992).

In addition to variation in morphological stage, there is size variation as well. Volumetric variation between embryos in mouse litters has been documented from about day 5 postcoitum through to birth (Goedbloed, 1972) but these data were not related to corresponding changes in morphology.

The most detailed account of mouse gastrulation to date has been provided by Theiler (1989). Between the time of the formation of the primitive streak to early organogenesis, Theiler recognized four stages of mouse gastrulation. However, he provided little detail concerning the morphological landmarks that define these stages of gastrulation, and he paid no attention to size and/or stage variation within litters. Recently, Fujinaga et al. (1992) adapted Theiler's staging system to rat gastrulation and proposed an extended numbering system for stages of gastrulation. Because rodent embryos exhibit considerable variation between strains, we feel that this classification system by numbers is too fixed with regard to the sequential and combinatorial landmarks of gastrulation; a description of stage by a combination of landmarks would be more immediately comprehensible.

Lawson and Pedersen have subdivided the early postimplantation embryo into six stages of embryogenesis, from the Pre-Streak stage to the Headfold stage (1987, see footnote to their Table 1). Although well-organized, it is only a footnote to a paper on cell lineages; there is not

enough detail to permit workers to easily recognize the various stages.

In the present study, we have attempted to establish a generally useful guide to the gross classification of mouse embryos during removal from their implantation sites, following reflexion of Reichert's membrane. We have determined the size variation within and between embryos, and have correlated size with trends in stage. We have maintained the three major stages described by Lawson and Pedersen (1987): Primitive Streak, Neural Plate and Headfold, but have expanded the Neural Plate and Headfold stages to take into account changes in the length and visibility of the head process, the presence and length of the allantoic bud and formation of the foregut. Thus, we have been able to place gastrulating embryos into nine groups.

For convenience, we often use the term 'stage' to classify embryos according to the morphological landmarks outlined, but we wish to be entirely clear in our meaning: while the landmarks described are common to all gastrulating embryos, their timing of appearance may be strain-dependent, leading to combinatorial differences. Thus, it is hoped that these landmarks will be applied flexibly by other investigators to describe their own mouse strains.

We have not sectioned our material for two reasons. (1) Our system is meant to be practical at the gross level, in order to expedite the sorting of a litter of embryos before processing. Should the stage of the embryos require closer scrutiny, those embryos should be further processed by sectioning, where any doubts about fine morphological features will be revealed. (2) Because whole-mount immunocytochemistry and whole-mount detection of mRNA expression is becoming more widely used and necessary in certain situations (Herrmann, 1991; Yamaguchi et al., 1992), embryos will not always be sectioned and staging will depend more on gross morphology.

Finally, we wish to emphasize that we have examined only one random-bred mouse strain and recognize that the timing of appearance of these landmarks of gastrulation may vary between strains (see, especially, the appearance of the allantoic bud within the posterior amniotic fold, Kaufman, 1991). Therefore, it is up to the investigator to be familiar with the timing of appearance of these markers in their own routinely used rodent strains and to employ combinatorial landmarks to classify embryos.

MATERIALS AND METHODS

PO (Pathology, Oxford) mice, a random-bred closed colony of albino mice, were used in this study. Pairs of oestrus females were chosen according to Champlin et al. (1973) for mating with one male per cage just before the beginning of the dark cycle (13.00 to 23.00). We used the midpoint of the dark cycle to standardize all dissections. We began our dissections at nominal day 6.75 postcoitum and assessed size and morphological stage at 0.25 day (6-hour) intervals until 8.0 dpc.

36 females were killed by cervical dislocation and used in this study. 3/36 litters showed signs of resorption (>25% resorptions) and were not analyzed further. Embryos from the remaining 33 litters were dissected for analysis. 387 implantation sites were found (average number of implantation sites per female was 11.4,

s.e.m.: 0.45); of these, 16 sites (4.1%) were in a state of resorption and 6 (1.6%) sites bore two embryos. Thus, 365 embryos were subjected to reflexion of Reichert's membrane and analysis. During reflexion, 63 embryos (17.3%) were damaged and discarded, leaving 302 embryos for this study.

Embryos were removed from their implantation sites as described in Hogan et al. (1986), in a modification of Dulbecco's Modified Eagle's Medium (DMEM) plus 7.5% fetal calf serum (FCS) (DMEM from Gibco Laboratories, UK; FCS from Flow Laboratories, UK; modification described in Lawson et al., 1991). Reichert's membrane was then reflected with the aid of sharp forceps and a 27-gauge hypodermic needle fitted to a 1 ml syringe or with glass needles according to Cockroft (1991).

Only one of the investigators measured the embryos in order to maintain consistency of error. Except for 7.25 dpc, all embryos were measured immediately after dissection. Embryos dissected at 7.25 dpc were fixed for several hours in 4% paraformaldehyde and rinsed in PBS for measurement. In separate experiments, we determined that there is no shrinkage of embryos during this brief fixation period.

The embryonic portion of all embryos was measured by the aid of a micrometer eyepiece. Pre-Streak embryos were measured in length from their point of constriction at the embryonic/extraembryonic junction ('circumferential groove') to their distal tip. The extraembryonic portion of some embryos was measured from this constriction to the insertion of the ectoplacental cone (Fig. 1A). The embryonic width was determined to be the greatest width of the embryonic portion. The embryonic portion of embryos at all other stages was measured from the anterior cranial limiting furrow to the distal tip and the extraembryonic portion from the cranial limiting furrow to the insertion of the ectoplacental cone (Figs 1B ,C ; 6B). Mesoderm was measured down the length of the posterior side only during Early Streak and Mid-Streak stages, using the anterior cranial limiting furrow as the proximal border of the embryonic portion (Fig. 1B ,C).

Staging of embryos was performed by rolling the embryos around with the aid of fine forceps and, except for Pre-Streak embryos where the posterior was not yet apparent by the primitive streak, examining them (1) on their left and right sides; (2) frontally, with the anterior pointing uppermost; and (3) in rear view, with the posterior end uppermost.

Embryos were viewed by both epi- and trans-illumination on a Wild M5 dissecting microscope with both ×10 and ×20 eyepieces and fixed objectives (×6-×50) and photographed on a Wild M8 microscope using Kodak TMax100 black-and-white film and processed according to the manufacturer's instructions. Embryos are shown on the same scale in Figs 1, 4 and 6 so that direct comparisons of size can be made.

RESULTS

(A) Criteria used to classify gastrulating embryos

We present here a set of morphological criteria for classifying gastrulation-stage embryos at the resolution of the dissecting microscope, from just before formation of the primitive streak (approximately 6.75 dpc) until the beginning of organogenesis at approximately 8.0 dpc, for a single, non-inbred strain of mice.

We have identified nine classification stages, adopting the staging system of Lawson and Pederson (1987) for the Pre- and Primitive Streak stages, but we have subdivided the Neural Plate and Headfold stages to take into account the presence of the allantois, a conspicuous feature of gastrula-
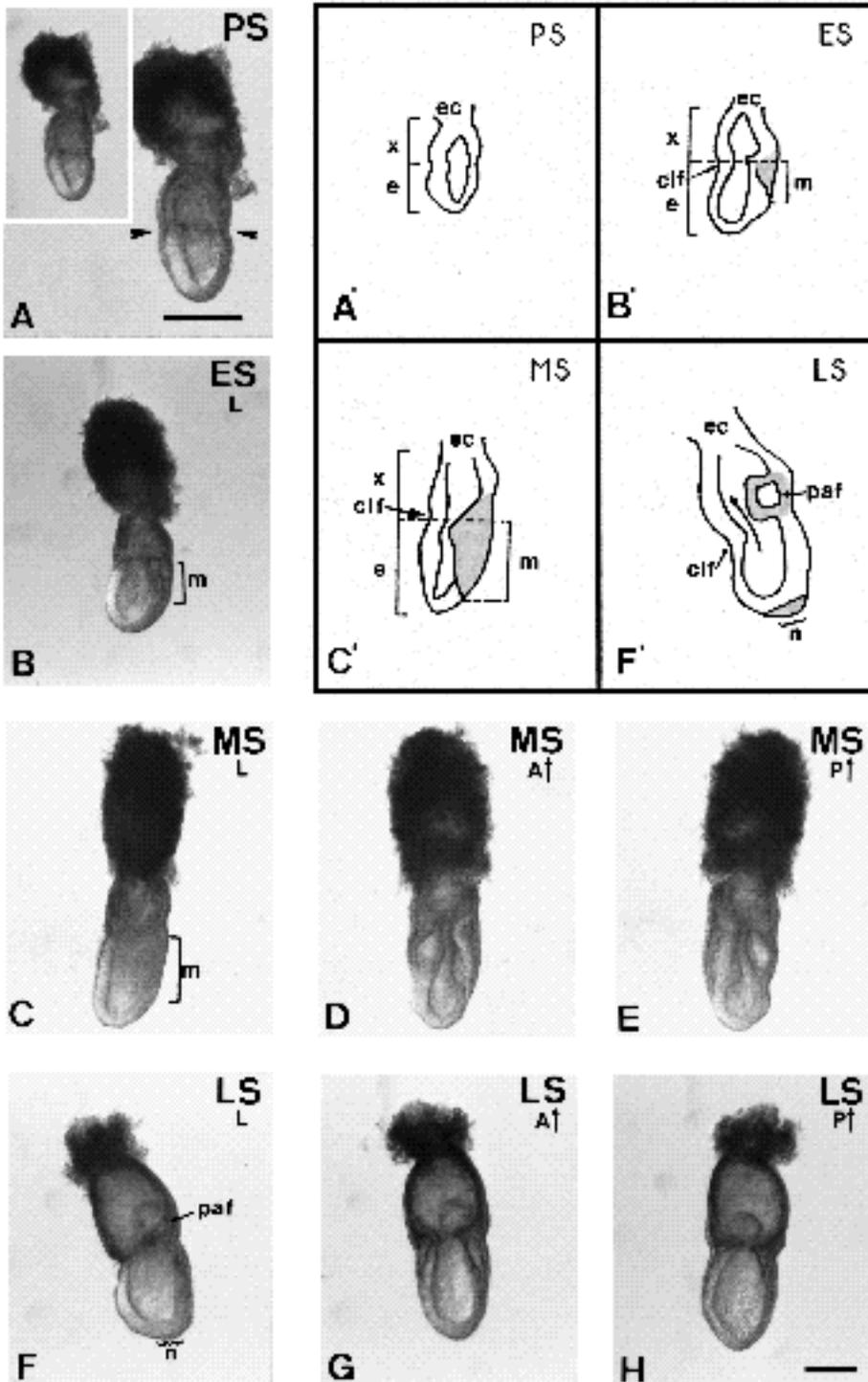
Fig. 1. Primitive Streak stages.(A) Pre-Streak stage; (B) Early Streak stage; (C) Mid-Streak stage; (F) Late Streak stage. All embryos, except the larger one in A, are on the same scale, indicated in H, where the scale bar = 200 µm. The scale bar in A is for the enlargement and is equal to 200 µm. All lateral views in this figure (B, C and F) and Figs 4 and 6, depict the posterior side of the embryo on the right, the embryo lying on its right side. For a complete description of anatomical features, consult Theiler (1989) or Kaufman (1992). (A) Pre-Streak (PS) stage. The solid arrowheads point to the circumferential constriction delineating embryonic and extraembryonic portions of the egg cylinder. This embryo has already begun to show signs of bilateral asymmetry, evident by a thickening in the embryonic ectoderm at the left and by a flattening of the egg cylinder. (B) Early Streak (ES) stage, lateral view. The bar at the posterior side delineates the extent of the embryonic mesoderm (m). (C-E): Mid-Streak (MS) stage. (C) Lateral view. (D) A͡. (E) P͡. (F-H): Late Streak (LS) stage. (F) Lateral view. The node (n) is at the distal tip. (G) A͡. (H) P͡. (A′, B′, C′, F′): Corresponding schematic drawings of the embryos shown in A-C and F. The bars to the left in A′, B′ and C′ indicate the method by which these embryos were measured (see Materials and Methods for details). The horizontal bar across the embryo and connecting to the bar on the right (B′, C′) shows how the embryonic mesoderm (m) was measured from the point of the cranial limiting furrow. The grey color indicates the distinctive features of each stage: (B′) ES: mesoderm extending up to 50% of the posterior side. (C′) MS: mesoderm extending between 51 and 100% of the posterior side; ratio of e:x approximately 2:1 (see Table 1). (F′) LS: posterior amniotic fold not yet fused to anterior proamniotic fold (the latter structure is not easily visible in the dissecting microscope) to form the amnion; the interior of this fold is the future exocoelomic cavity; node condensed and visible. The arrow between the embryonic and extraembryonic portions is the proamniotic duct. **Abbreviations used in all figures**: ab, allantoic bud; al, allantois; am, amnion; A͡, anterior upwards; clf, cranial limiting furrow; e, embryonic portion of egg cylinder; ec, ectoplacental cone; etc, ectoplacental cavity; fg, foregut; hf, headfolds; hp, head process; L, lateral view; µm, micrometer; m, embryonic mesoderm; n, node; nec, neurectoderm; ng, neural groove; np, neural plate; P͡, posterior upwards; paf, posterior amniotic fold; x, extraembryonic portion of the egg cylinder; xc, exocoelomic cavity.

tion, and the formation of rudimentary headfolds. The criteria used to identify and arrange these stages are described below and are summarized in Table 1 and schematically in Figs 1, 4, 6 and 9. Consistent morphologi-

cal characteristics of embryos at each stage are highlighted in bold type in Table 1.

Based on this classification system, variation amongst the litters is shown in Table 2. At most times of dissection, at

Table 1. Classification of embryonic stages

	Pre-Streak	Primitive Streak			Neural Plate			Headfold	
	PS	ES	MS	LS	OB	EB	LB	EHF	LHF
Mesoderm	**no**	**to 50% posterior**	**to 100% posterior**						
Node (formerly, head process, which includes the midline extension anterior from the node; archenteron)	no	no	no	**exposed at dt[1] and may extend anteriorly**	hp extended anterior to dt and visible	hp extended anterior to dt and visible	hp not visible; node may be visible as slight depression near dt	**node may be visible anterior to dt, and crescent-shaped**	**node anterior to dt, and crescent-shaped**
Amnion	no	no	no	**paf[2] visible**	**paf closed**	closed	closed	closed	closed
Cavities	1	1	1	1	**3**	3	3	3	3
Allantois	no	no	no	no	**no**	**small**	**larger, may/may not be adherent to wall**	**slender at tip and projecting freely into exocoel. cav.**	
Neurectoderm	no	no	no	no	neural plate just forming	**neural plate edges defined**	neural groove may be visible	**neural groove visible**	**headfolds**
Foregut	no	no	no	no	no	no	no	no	**present**
Ratio[3]: Emb L: Emb W	1.03±0.02 (55)[4]	1.17±0.03 (39)	1.18±0.03 (51)	1.20±0.03 (23)	1.08±0.02 (21)	1.07±0.02 (18)	0.94±0.02 (26)	**0.79±0.02 (30)**	**0.86±0.03 (16)**
Ratio[3]: Emb L: Extraemb L	1.15±0.05 (18)	1.50±0.07 (30)	**1.86±0.07 (36)**	1.38±0.07 (17)	1.17±0.05 (12)	1.18±0.06 (18)	1.02±0.03 (26)	1.19±0.06 (30)	1.27±0.19 (6)

[1]dt=distal tip (see text).
[2]paf=posterior amniotic fold.
[3]The ratios are reported as means±s.e.m.s.
[4]Numbers in parentheses are the numbers of embryos scored.

least three different stages could be found and sometimes as many as five (see footnote to Table 2).

The primitive streak, which (1) signals the onset of gastrulation, (2) defines, by its appearance, the posterior end of the embryo and (3) forms the anteroposterior axis, by elongation through the midline of the egg cylinder, is a most important feature and forms the basis of staging embryos until it reaches just beyond the distal tip of the egg cylinder. Thus, we will consider first those embryos without a primitive streak.

Pre-Primitive Streak stage
(1) Pre-Streak (PS) (6.75-7.25 dpc)
The distinguishing characteristics of Pre-Streak embryos are highlighted in bold type in Table 1 and are described below. A typical Pre-Streak embryo is shown in Fig. 1A and 1A . All such embryos showed the following features.

(a) Clearly distinct embryonic and extraembryonic ectoderm, distinguished by a circumferential constriction ('circumferential groove') of visceral endoderm.

(b) A proamniotic cavity that was continuous between the embryonic and extraembryonic portions. (The size of the proamniotic cavity was not considered in this study.)

(c) No evidence of mesoderm.

Mesoderm is unequivocally absent from Pre-Streak embryos and unequivocally visible in Early Streak embryos (see below). However, there appears to be a transitional stage when the primitive ectoderm breaks down to form the primitive streak; the embryo is flatter on two sides and the circumferential groove does not span the entire perimeter of the embryo, but is transformed into the cranial limiting furrow (see Fig. 1B'). We could not find evidence of mesoderm. These embryos may be transitional embryos and for practical studies, we call them PS/ES embryos (see Table 2).

Pre-Streak (PS) embryos were found at three dissection points: 6.75, 7.0 and 7.25 dpc (Table 2). At 6.75 dpc, the majority of embryos did not have an obvious primitive streak (72.1%), as judged by the absence of a small wedge of mesoderm (see Fig. 1B, Early Streak), but, by 7.0 dpc, fewer than half the embryos were classified as Pre-Streak (35.9%). The range in stage within litters is given in Table 2.

Primitive Streak stages
(2) Early Streak (ES) (6.75-7.25 dpc)
Early Streak embryos were classified by this single most important characteristic: a small wedge of mesoderm, which was just visible or extended up to 50% the length of the posterior side (Table 1). A representative Early Streak (ES) embryo is shown in Fig. 1B,B .

Classifying Early Streak embryos can be somewhat difficult, because the small wedge of mesoderm, though present, may be very difficult to discern under the light microscope (see Discussion in previous section). Also, size alone cannot be used as Fig. 2 shows considerable overlap

Table 2. Stage variation between litters

	6.75d (5)*	7.0d (7)	7.25d (5)	7.5d (5)	7.75d (5)	8.0d (6)
PS	31/43 (72.1%)	23/64 (35.9%)	1/47 (2.1%)			
ES	11/43 (25.6%)	19/64 (29.7%)	10/47 (21.3%)			
MS		16/64 (25.0%)	33/47 (68.8%)	13/43 (30.2%)	3/47 (6.4%)	
LS			1/47 (2.1%)	9/43 (20.9%)	13/47 (27.7%)	
NP/OB			2/47 (4.2%)	10/43 (23.2%)	9/47 (19.1%)	
NP/EB				3/43 (7.0%)	13/47 (27.7%)	2/58 (3.4%)
NP/LB				3/43 (7.0%)	6/47 (12.8%)	17/58 (29.3%)
EHF				5/43 (11.6%)	3/47 (6.4%)	22/58 (37.9%)
LHF						16/58 (27.6%)
Somites						1/58 (1.7%)†
PS/ES	1/43 (2.3%)	6/64 (9.4%)	0	0	0	0

*Numbers in parentheses represent the number of litters assessed.

†This embryo had 5 somites and the allantois was fused to the chorion.

The broken vertical line linking stages indicates the least number of stages found; except for 7.75d, all litters contained at least one damaged and thus, unscored embryo.

The solid vertical line linking stages indicates the widest range of stages found within single litters. This line does not take into account damaged and thus, unscored embryos.

found in size between the PS and ES stages. We could not be sure of the classification of 11.7% of all embryos examined at 6.75 and 7.0 days because mesoderm was not visible in these embryos, although they showed marked bilateral asymmetry; therefore, we classified them as PS/ES embryos (see Table 2).

(3) Mid-Streak (MS) (7.0-7.75 dpc)
Mid-Streak (MS) embryos were comparatively easy to classify. The length of the primitive streak (as judged by the extent of mesoderm down the posterior side) was between 51 and 100%, and its spreading mesodermal 'wings' could extend laterally to the midline of the left and right sides of the nascent embryo, sometimes obscuring the outline of the underlying primitive ectoderm (Fig. 1C,C). Importantly, in cases where the primitive streak had reached the distal tip, it had not yet condensed into a visible head process. Also, the ratio of embryonic to extraembryonic ectoderm was significantly different from all other stages, being 1.86±0.07 as compared to 1.02±0.03 to 1.50±0.07 (Table 1; Tukey's test for multiple comparisons using a significance level ('error rate') of 0.05), though this feature on its own is not enough to classify these embryos as other stages were sometimes within the limits of this proportionality.

When rolled from its side (with respect to the primitive streak) so that the anterior or posterior side was facing up, the mesoderm wings were obvious, occluding the underlying primitive ectoderm over which they had spread (Fig. 1D,E).

Mid-Streak stage embryos could be found at four dissecting periods, from 7.0 dpc litters to 7.75 dpc litters, but were most frequently observed at 7.25 dpc (68.8%, Table 2). That they can be found at 7.75 dpc emphasizes once again the urgency of reporting morphological landmarks in gastrulating embryos, because some investigators choose the Headfold stage embryo as representative of this postcoital age of dissection (see, for example, Herrmann, 1991). Our material shows that, at 7.75 dpc, there is no predominant stage; Early Headfold stage embryos are present but constitute only 6.4% of the embryos dissected at this timepoint (Table 2).

(4) Late Streak (LS) (7.25-7.75 dpc)
Lawson and Pedersen (1987) have proposed that, consistent with the staging system of the chick, gastrulating mouse embryos be staged according to the length of the primitive streak and designated as Early, Mid- and Late Streak embryos. In Late Streak embryos, the anterior end of the primitive streak condenses into the 'node' at the distal tip of the egg cylinder; this structure is generally believed to be
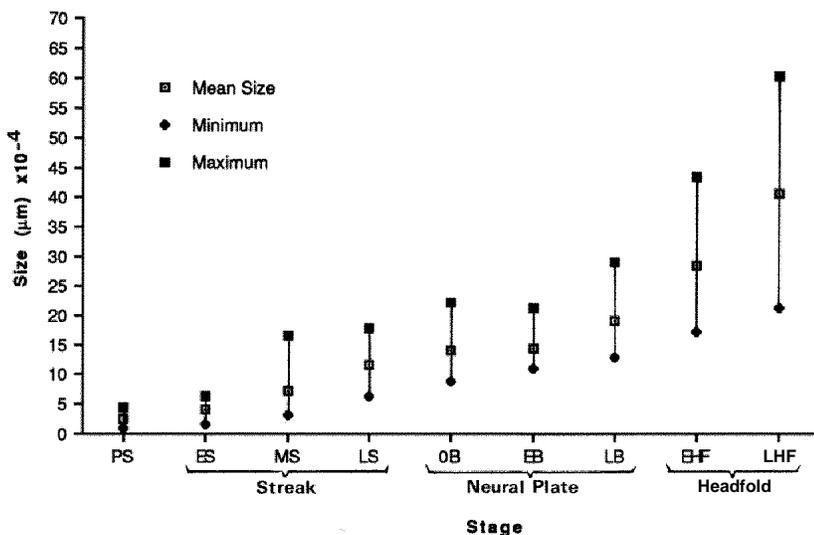
Fig. 2. Mean size of gastrulation stage embryos. Embryos were staged according to the details in the text and the embryonic portion of each embryo was measured as described in Materials and Methods. The embryos were plotted by stage (X-axis) against size (10^{-4} μm, Y-axis). The mean is given by the open squares and the maximum and minimum sizes by the closed squares and diamonds, respectively. The means ± s.e.m.s (in 10^4 μm) are PS: 2.38±0.09; ES: 4.02±1.6; MS: 7.15±0.30; LS: 11.64±0.54; OB: 13.98±0.71; EB: 14.39±0.68; LB: 18.94±0.89; EHF: 28.34±1.46; LHF: 40.48±2.55.
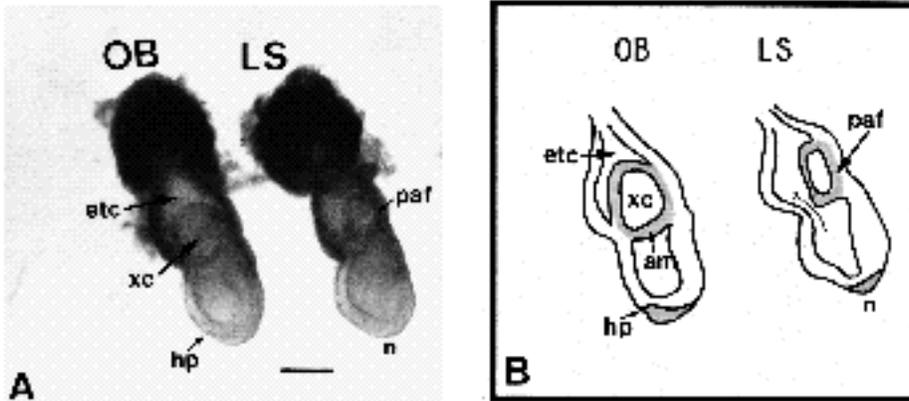
Fig. 3. Comparison of Late Streak stage and No Bud stage embryos. (A) Lateral views of 'No Bud' (OB) stage embryo is shown on the left and the Late Streak (LS) stage embryo on the right. Note the full closure of the amnion in the 0B stage embryo and expansion of the exocoelomic cavity (xc) as compared with the LS stage embryo. The third, ectoplacental cavity (etc), is often not visible in whole embryos. The distalmost arrows in A and B indicate the anteriormost extent of the head process (hp). Scale bar, 200 μm. (B) Schematic drawing highlighting in grey the important comparative features of these two embryos: OB: full closure of the amnion and formation of the exocoelomic cavity (xc, left) and anterior midline extension of the node to form the head process. LS: the persistance of the posterior proamniotic fold and lesser extension of the node. The arrow in B in the LS embryo indicates the proamniotic duct.

equivalent to Hensen's node in the chick and is also called the 'archenteron' when the embryos have reached the Headfold stage. (At a recent Ciba Symposium on Post-Implantation Mouse Development, it was suggested (Beddington, 1992) that 'archenteron' be abandoned and that the anterior point of condensation of the primitive streak be called the 'node'.)

By the criteria of Lawson and Pedersen (1987), Late Streak embryos bear a condensed node (the anteriormost part of the primitive streak and located at the distal tip of the embryonic portion of the egg cylinder) which is 'exposed' at the distal tip (Fig. 1F,F), and is correlated with rupture of the endoderm at this point. The head process is an extension of the node, thus becoming a rostral extension of the primitive streak. It consists of tightly packed cells, which appear to be directly exposed to the yolk cavity because of the discontinuity in the overlying endoderm (for a description of the head process at the Late Streak stage, see Poelmann, 1981; for a description at the Headfold stage, see Jurand, 1974). The distinguishing contour of the head process can be seen very clearly in histological sections presented by Kaufman (1992; Plate 5a-d, and called the 'notochordal plate').

In addition to the diagnostic head process, an important feature of Late Streak embryos is the appearance of the posterior amniotic fold. Late Streak embryos were classified as to whether the posterior amniotic fold had closed to form the amnion (Table 1). In the material used by Lawson and Pedersen (1987), as well as in the PO strain in this study, Late Streak embryos did not bear closed amnions. Rather, the posterior amniotic fold appeared to be just in the process of coalescing with the smaller fold of the anterior side (Fig. 1F,F and see the comparison between LS embryos and those without an allantoic bud but with three complete cavities, Fig. 3). The 'proamniotic duct' acts as a conduit between the proamniotic cavity and the ectoplacental cavity until amnion formation is complete.

The ratio of the embryonic ectoderm to extraembryonic ectoderm has decreased (Table 1). In contrast to Lawson and Pedersen, we did not use the extent of mesodermal spread over the primitive ectoderm as a diagnostic feature of this stage, because it was difficult to detect in all embryos, although in some specimens examined, the mesoderm obviously extended to the midline of the egg cylinder, as indicated by these authors.

Neural Plate stages (NP)

(5) No Allantoic Bud (OB) (7.25-7.75 dpc)

The next three substages that we describe are encompassed within the Neural Plate stage, described by Lawson and Pedersen. We have subdivided this stage to take into consideration the appearance and size of the allantois, the visibility of the head process and the form of the anterior ectoderm, which will become the headfolds.

In the Neural Plate/No Allantoic Bud substage (OB), the posterior amniotic fold has fused with the less distinct anterior amniotic fold to form a complete amnion and three cavities instead of one: the amniotic cavity (formerly, 'proamniotic cavity' before amnion closure, and generally visible in whole embryos), the exocoelomic cavity (generally visible in whole embryos), and the ectoplacental cavity (not often visible in whole embryos). No allantoic bud was visible and we designate this substage as 'No Allantoic Bud' (OB; Fig. 4A-D). This stage has also been depicted in Beddington (1983, Fig. 1.1e).

We have compared a Late Streak (LS) embryo with an embryo in which the amnion has just closed and no bud has yet formed (OB) (Fig. 3) in order to show the most obvious difference between these two stages, namely, the appearance of a complete exocoelomic cavity in the case of the OB and the presence of the posterior amniotic fold in the LS embryo. In both embryos, the head process is visible, but the extent of its anterior displacement is not a diagnostic feature (Figs 3A, 4A,B). Also, there is evidence of neural groove formation in the distal half of the embryonic portion of the egg cylinder in the OB stage embryo when placed anterior and posterior sides up (Fig. 4C,D).

(6) Early Allantoic Bud (EB) (7.5-8.0 dpc)

In Early Allantoic Bud embryos, a small allantoic bud could be seen at the posterior junction of the embryonic and extraembryonic portions of the egg cylinder, lying at the

junction of the amnion with the extraembryonic mesoderm (Fig. 4E-H). In most cases, it could best be seen by rolling the embryo so that its posterior side was facing upwards

(Fig. 4H). When rolled, either with its anterior or posterior side up, the edges of the neural plate were conspicuous, bordering the incipient neural groove, the node appearing as
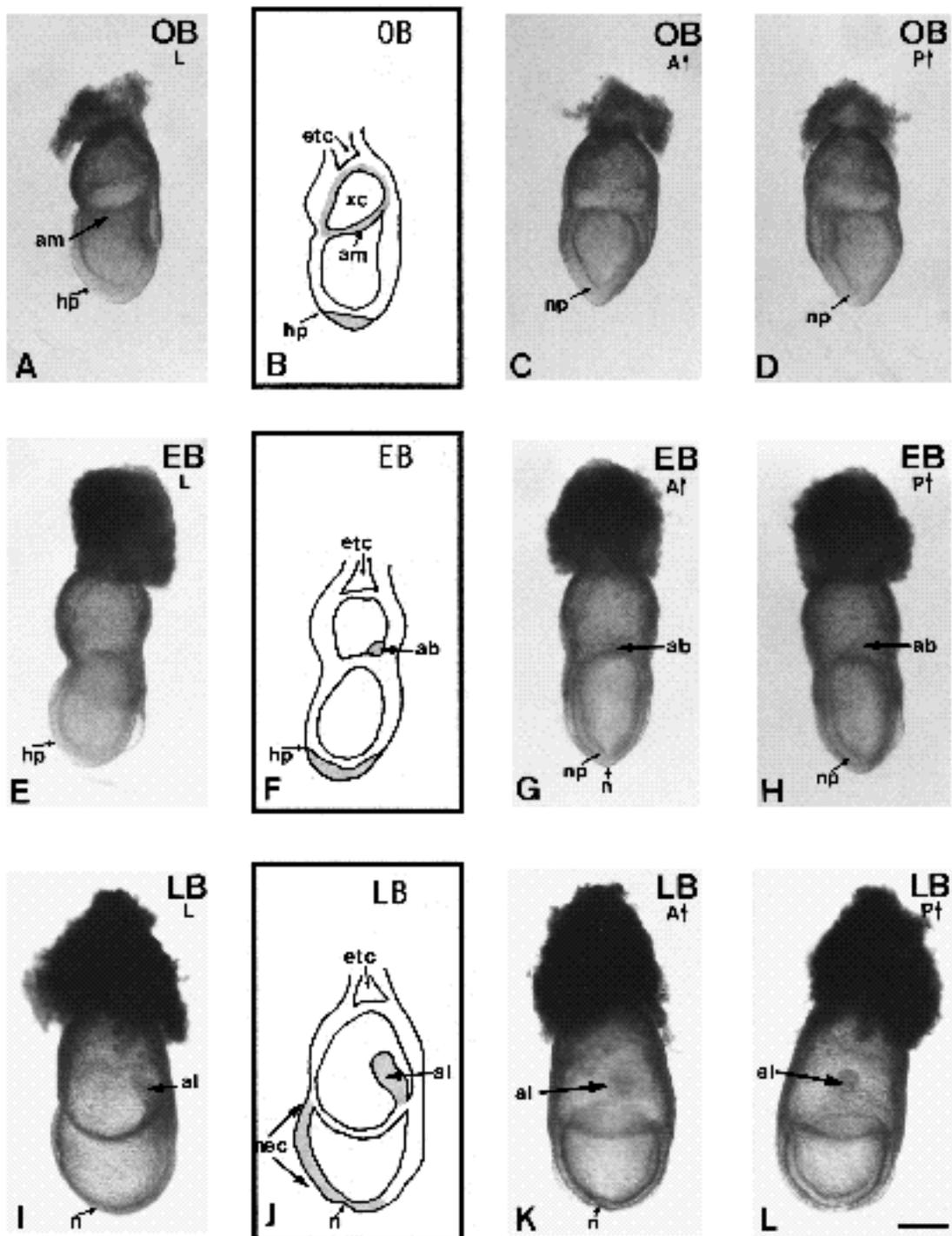
Fig. 4. Neural Plate: Allantoic Bud stages. As in Fig. 1, the lateral views (A,E,I) of all embryos are shown with posterior on the right, the embryos lying on their right side. The scale bar in L is 200 μm. (A-D) No Allantoic Bud (OBud); (E-H) Early Bud (EB); (I-L) Late Bud (LB). See list of abbreviations for explanation of anatomical structures. (C,G,K) A ; (D,H,L) P . (B,F,J) Schematic drawings indicating the important morphological landmarks (in grey) of these neural plate substages. (B) OB: extended head process (hp) and formation of the exocoelomic cavity (ec) by full closure of the amnion (am); (F) EB: extended head process and presence of a small allantoic bud (al) (though not visible in E, the allantoic bud can be seen when the embryos are rolled, as in G and H; (J): LB: larger allantois, projecting into the exocoelomic cavity, anterior neurectoderm (nec) thickening but not yet forming headfolds, node (n, formerly 'archenteron') is crescent-shaped (This last structure may not be easily visible in lateral view—see I).
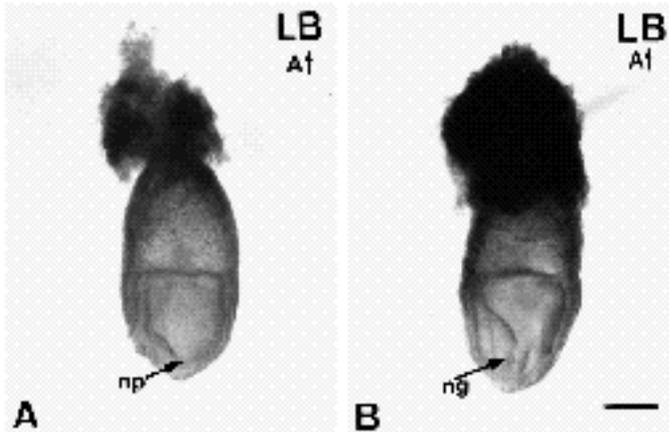
Fig. 5. Two LB embryos (A) to compare development of neural plate. (A) Neural plate (np) still visible; (B) neural groove (ng) just visible distally.

a 'knot' at the distal tip (Fig. 4G). The head process was still visible and extended anteriorly (Fig. 4E,F)

(7) Late Allantoic Bud (LB) (7.5-8.0 dpc)

By the Late Allantoic Bud substage, the embryo is becoming wider than it is long (Table 1). The length of the bud has increased (we did not consistently measure the bud because we could not be certain of the location of the base of the allantois) and generally projected into the exocoelomic cavity (Fig. 4I). The head process is no longer a distinct feature along the anterior midline of the embryo and does not have a distinct boundary. If the embryos are rolled frontally, with the anterior midline visible, an obvious neural groove may be, but is not always, discernible (Fig. 5A,B). Furthermore, the node (formerly, archenteron—see Discussion in the section on Late Streak Embryos) may be visible as a crescent-shaped depression (Fig. 4K).
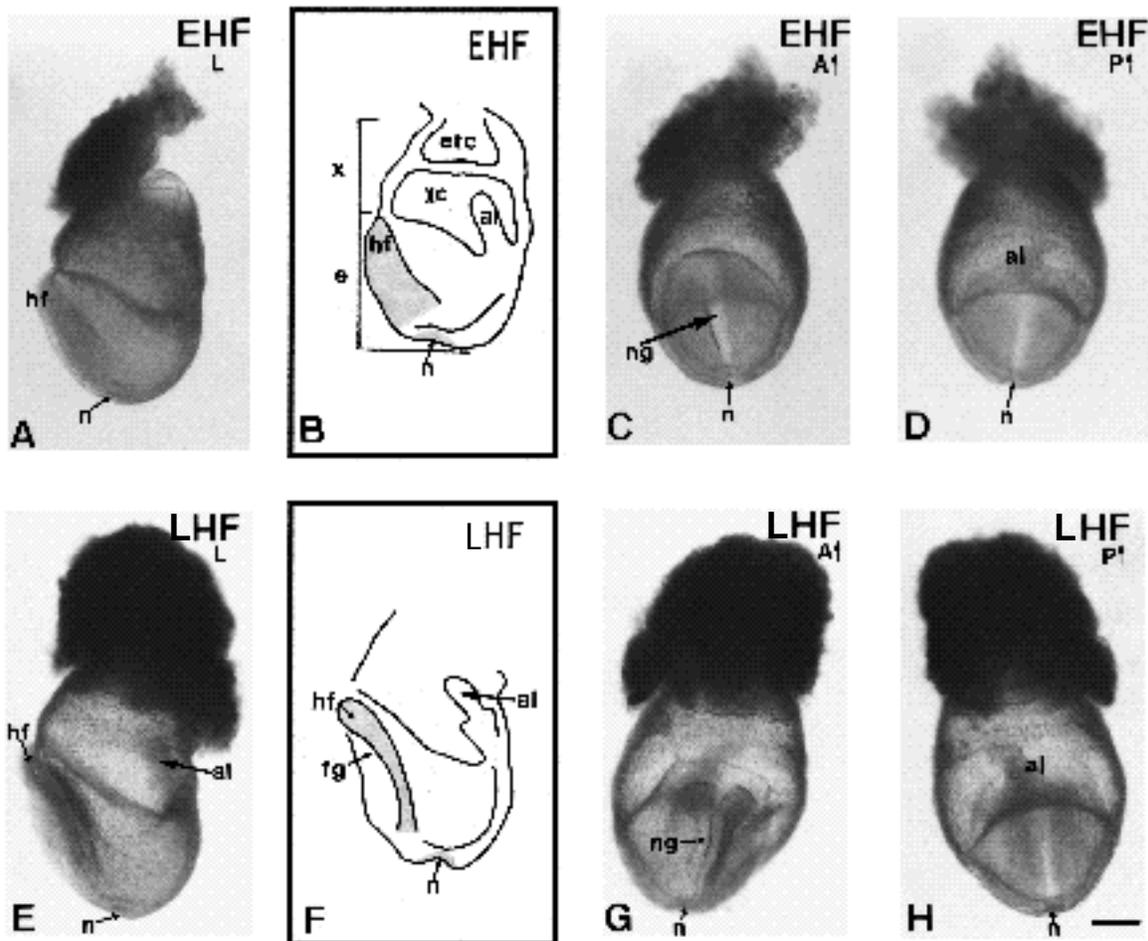
Fig. 6. Headfold stages. (A-D) Early Headfold (EHF) stage; and (E-H) Late Headfold (LHF) stage. (A,E): Lateral views; (C,G) A ; (D,H) P . See list of abbreviations in Fig. 1 for explanation of morphological landmarks. The scale bar in H corresponds to 200 μm. In C, the neural groove (ng) has not yet closed, whilst in G, the neural groove is closing and can be seen when anterior is uppermost. (B,F) Schematic drawings showing in grey the most important features of these stages: (B) EHF: anterior ectoderm thickening to form headfolds (hf). No foregut is yet visible. The node (formerly, archenteron) is visible and crescent-shaped just anterior to the distal tip. The bars on the left of the embryo show how measurements were carried out (see Materials and Methods). (F) LHF: the anterior neurectoderm has thickened to form distinct headfolds and a foregut pocket has become visible. The node is visible as a crescent-shaped feature slightly anterior to the distal tip.
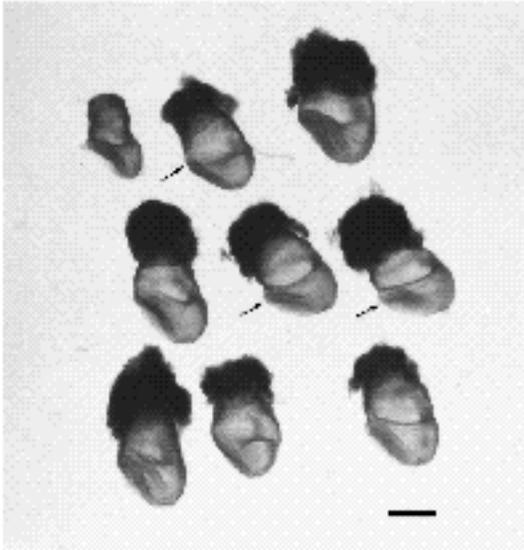
Fig. 7. 8.0 dpc litter showing variation in stage and size of EHF and LHF embryos. This litter is indicated in Table 2, 8.0d, by a solid line. One of the embryos was damaged and not scored, but the remaining 9 embryos fell into these two categories. Arrows point to EHF-stage embryos. They were classified as EHF because the head folds were not yet articulated and a foregut pocket was not visible. Scale bar = 500 µm.

Headfold stages

(8) Early Headfold (EHF) (7.5-8.0 dpc)

A more advanced stage, with an elongated allantois invariably projecting freely into the exocoelomic cavity and early neural groove formation anteriorly was found just before the overt Late Headfold stage. This stage did not show foregut invagination, as described for the Headfold stage by Lawson and Pedersen. Early Headfold embryos were more advanced than the previous Late Bud stage, because the allantois had grown and the anterior ectoderm was thickened and conspicuously sigmoidally curved (Fig. 6A). The node was generally slightly formed just anterior to the distal tip as a crescent-shaped depression and, when viewed frontally, the neural groove was distinct and obvious (Fig. 6A,C). Characteristically, the embryos at this stage differed significantly in their l:w ratio to those in the previous Neural Plate: LB stage (based on Tukey's test for multiple comparisons using a significance level (error rate) of 0.05; this ratio is not significantly different from the LHF stage, as determined by the same test). Although the l:w ratio for LB and EHF is significantly less than 1.0 (*t*-test, 0.05 level), the deviation from 1.0 is more pronounced in the EHF stage.

(9) Late Headfold (LHF) (8.0 dpc)

Late Headfold stage embryos bore obvious and well-defined headfolds, the neural groove was present in the anterior midline of the embryos when viewed frontally, and the foregut pocket was forming just below the headfolds (Fig. 6E-H). The node was conspicuous distally (Fig. 6E). An example of a single litter of Headfold stage embryos is found in Fig. 7. This litter demonstrates that not all embryos at the same stage of development are the same size.
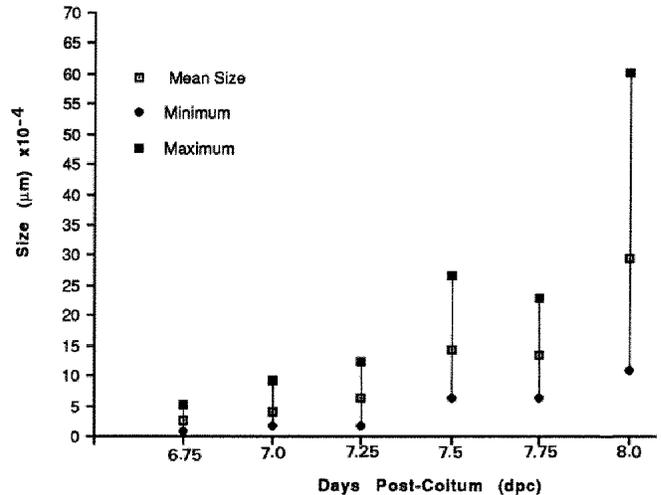
Fig. 8. Mean embryo size (at dpc). At each time point, embryos from 5-7 litters were measured (see Table 3 for each litter size, average litter size and s.e.m.s), and the mean (open squares) taken for all embryos (Y-axis). The maximum and minimum embryo sizes for each time point are reported as closed boxes and diamonds, respectively.

Somite stages

(10) Somite stage embryos (8.0 dpc and beyond)

We have not set out in this study to characterize embryos with somites (for staging rat embryos at the onset of early organogenesis, see Brown and Fabro, 1981). We found, however, a single embryo dissected at 8 days with five somites and chorioallantoic fusion occurring, an event that generally begins at the 5-somite stage in the PO strain (K. Downs, unpublished).

(B) Variation in embryo size within and between litters

The dimensions of the length of the embryonic portion multiplied by its width were calculated as a gross indication of embryo size. The embryonic portion of the egg cylinder was chosen because it constitutes the entire nascent fetus. Similar results were obtained when the entire conceptus was used (data not shown). It is clear that there is enormous size variation amongst embryos within and between litters (Fig. 8 and Table 3). We observed very little difference in overall size of embryos in the 6-hour interval between 7.5 and 7.75 dpc, when embryonic growth may be slowing, though without left-right measurements, we cannot be certain that litters at 7.75 days are, in fact, larger.

The measurements we obtained for the PO Swiss-derived strain are in close agreement with those reported recently by Lawson and Pedersen (1992) for non-inbred Swiss mice.

(C) Correlation between embryo size and stage of development is not absolute

Fig. 2 shows the relationship between embryo size and morphological stage, as determined by the landmarks described above. It is clear from these data that size and stage are linked, as there is a general trend toward increased size as more advanced stages are attained. However, the corre-

Table 3. Mean embryo sizes ± s.e.m.s for individual and total litters

	6.75 days	7.0 days	7.25 days	7.5 days	7.75 days	8.0 days
Litter 1	1.70±0.11* (8)†	2.37±0.16 (11)	4.94±0.56 (9)	8.34±0.43 (8)	10.05±0.60 (10)	17.31±1.06 (12)
Litter 2	2.39±0.16 (12)	2.96±0.39 (10)	5.27±0.40 (11)	12.0±0.62 (10)	12.24±0.63 (9)	25.31±3.14 (9)
Litter 3	2.52±0.08 (6)	3.87±0.36 (9)	5.79±0.35 (9)	13.42±1.16 (6)	14.67±1.42 (9)	28.25±3.22 (8)
Litter 4	2.54±0.26 (11)	3.98±0.33 (5)	6.21±0.84 (7)	18.01±1.72 (8)	14.99±1.18 (9)	29.73±2.62 (11)
Litter 5	4.32±0.35 (6)	4.26±0.40 (12)	8.88±0.73 (11)	18.18±1.12 (11)	15.90±1.36 (10)	35.13±2.27 (9)
Litter 6		4.42±0.24 (10)				45.49±3.06 (9)
Litter 7		7.2±0.66 (7)				
Total	2.59±0.15 (43)	4.00±0.22 (64)	6.29±0.33 (47)	14.22±0.75 (43)	13.54±0.57 (47)	29.55±1.53 (58)

*All numbers are expressed in 10^4 micrometers (μm; see Methods).
†Numbers of embryos per litter (see Methods).

spondence is not precise, as we found embryos of similar size that were at different stages of development.

We observed little difference in size between the fetal portions of embryos classified as OB and EB, both in growth of the fetal portion of the egg cylinder and overall egg cylinder size (using t-test with 0.05 significance level) so that, at least initially, the growth of the allantois is not correlated with overall embryonic growth.

DISCUSSION

Precise staging of embryos during gastrulation is essential in order to achieve comparability within and reproducibility between all studies undertaken during this time window. We have presented a set of morphological landmarks for classifying gastrulating mouse embryos in a dissecting microscope, with the aim of providing a more precise method that is not subject to the confounding factors of variability between littermates of the same litter, between litters, lighting regimes, etc., when reporting embryonic stage. The importance of this guide rests on the fact that the stages of mouse embryos within a single litter are highly variable. Because of recent technical advances that entail hybridization to mRNA and protein localization, it is imperative that a consensus of morphological landmarks be reported so that data can be more uniformly interpreted. To demonstrate the utility of our system, the morphological landmarks reported in this study can be applied to, for example, the *Brachyury* whole-mount in situ expression patterns in the gastrulating mouse (Herrmann, 1991), where the staining patterns overlap with morphological landmarks that we have described (Fig. 1A-E: MS, LS, LB, EHF and LHF, respectively). (See also Beddington et al., 1992, Fig. 1A: ES; Fig. 1B: Neural Plate/LB.)

By dissecting embryos with respect to the midpoint of their dark cycle and carrying out simple measurements, we have shown formally that (1) embryos within and between litters differ significantly in overall size; (2) embryonic stage is highly variable within and between litters; and (3) although growth and morphogenesis are linked, they are not

closely correlated. Furthermore, we have refined the briefly described staging system of Lawson and Pedersen (1987), forming, thus, nine classification categories.

It must be emphasized that we have analyzed only a single random-bred mouse strain. We have described those landmarks that are consistent and obvious morphological features of mouse gastrulation, and which ought to be reported when describing gene expression patterns. It is conceivable that the sequence of appearance of landmarks in other strains may be out of synchrony with the Swiss-derived strain characterized here (see below, 'The Allantois as a Morphological Landmark').

A summary of the diagnostic features of gastrulation can be found in Fig. 9.

The allantois as a morphological landmark

The allantois is an extraembryonic mesodermal outgrowth of the primitive streak. Its cellular and molecular nature are not well-characterized, although genes shown to be expressed in the extraembryonic allantois are not expressed in the derivative primitive streak and the embryonic mesoderm and vice-versa (see, for example, Downs et al., 1989; Wilkinson et al., 1990).

The development of the allantois, which subdivides the neural plate stage into three stages before the headfolds are identifiable, is a particularly important feature of our staging system but its timing of appearance appears to vary. Kaufman describes the origin of the allantois within the posterior amniotic fold well before fold closure (see Fig. 1B, Kaufman, 1990). We have found no evidence for the formation of an allantois until after closure of the amniotic folds (data not shown for 6 sectioned embryos). Thus, Swiss-derived mice probably differ from the (C57/Bl × CBA) F_2 embryos used by Kaufman. The differences in timing of allantoic bud formation for the F_2 hybrids and the non-inbred Swiss mice have been corroborated by K. Lawson (personal communication).

Other investigators have demonstrated no strong correlation between developmental stage and development of the allantois in presomite rat embryos (Fujinaga and Baden,
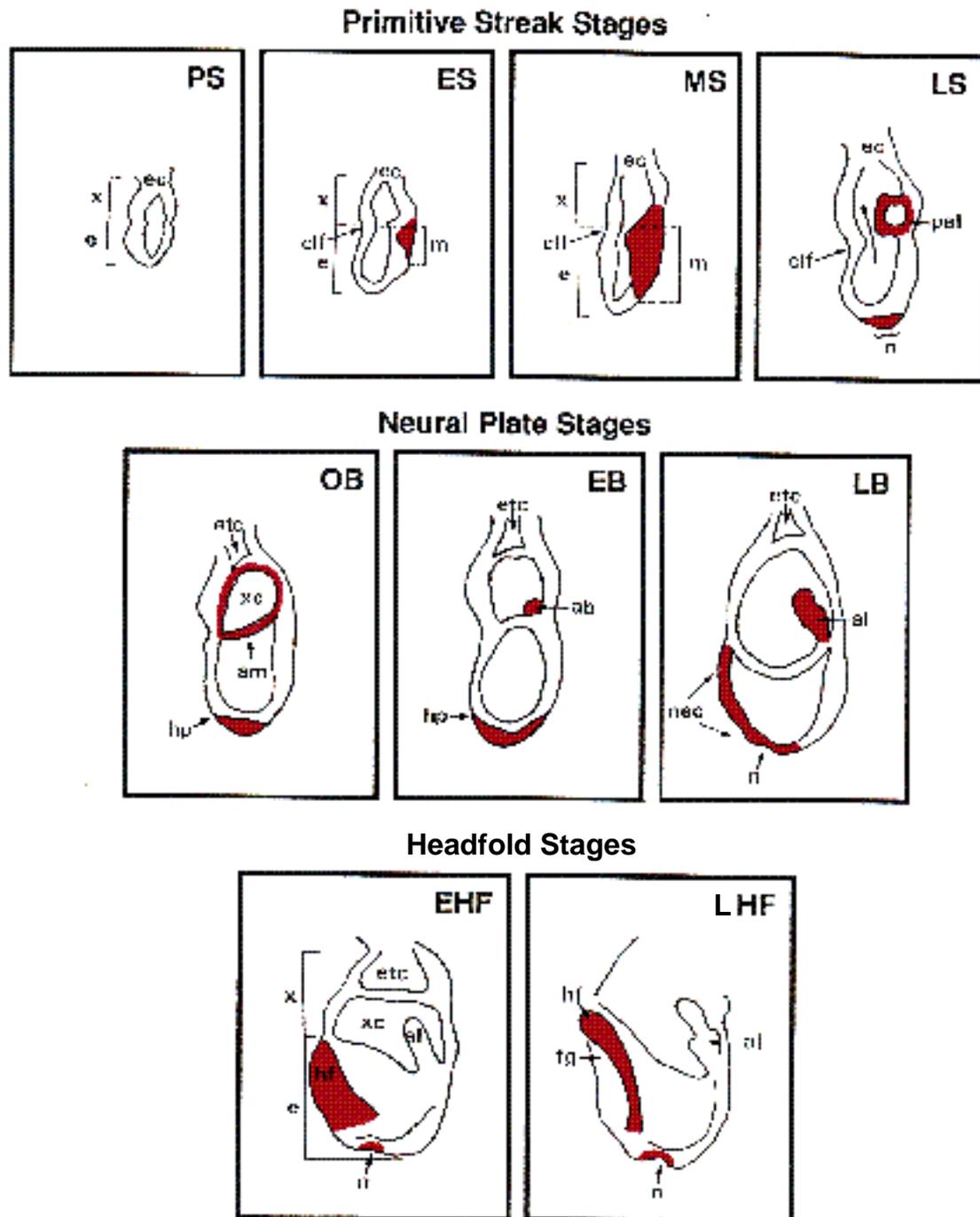
Fig. 9. Morphological landmarks of gastrulation. Summary of the important diagnostic morphological landmarks (in red) described in the text, Table 1 and the examples of living embryos in Figs 1, 4 and 6 (where their corresponding diagnostic features are schematized in grey). These features may vary according to Table 1 (e.g., the mesoderm in the MS embryo may extend up to 100% of the posterior side). Abbreviations as in Fig. 1.

1992). It is thus possible that extraembryonic development proceeds somewhat independently of embryonic development.

Although the allantois is a prominent feature of the Neural Plate Stage in our non-inbred Swiss mouse strain and is thus a useful gastrulating landmark for working with Table 1, we must emphasize that as its timing of appearance may be variable, its presence must be reported with relation to the other landmarks.

Variation within litters

The variation between embryos within litters is not fully understood. One factor documented to account for litter variability is the variation in developmental advancement

with the sex of the embryo: XY-bearing embryos develop faster than XX during preimplantation development (Tsunoda et al., 1985; Burgoyne, 1993). At postimplantation stages of development, males are still developmentally advanced relative to females, although there is no difference in rate of development at this time (Seller and Perkins-Cole, 1987; Brook et al., 1991). It has been suggested that differential imprinting of the X chromosomes after X-inactivation may account for the difference between the sexes (Thornhill and Burgoyne, 1993).

Conclusion

We have shown formally the extensive size and stage variation within and between litters of early postimplantation mouse embryos and suggest a series of morphological landmarks to be cited when sorting embryos for experimental purposes. It is hoped that these landmarks standardize studies in mouse gastrulation; careful reporting of combinations of landmarks should also identify the sequence of morphological differentiation essential to appropriate pattern formation during gastrulation.

REFERENCES

Beddington, R. S. P. (1983). The origin of the foetal tissues during gastrulation in the rodent. In *Development in Mammals*, Vol. **5** (ed. M. H. Johnson), pp. 1-32. Amsterdam: Elsevier Science Publishers.

Beddington, R. S. P. (1992). In *Post-Implantation Development in the Mouse. Ciba Foundation Symposium* **165** (ed. D. J. Chadwick and J. Marsh), p. 55. Chichester: Wiley.

Beddington, R. S. P., Rashbass, P. and Wilson, V. (1992). *Brachyury* - a gene affecting mouse gastrulation and early organogenesis. *Development* **1992 Supplement**, 157-165.

Blum, M., Gaunt, S. J., Cho, K. W. Y., Steinbisser, H., Blumberg, B., Bittner, D. and DeRobertis, E. M. (1992). Gastrulation in the mouse: The role of the homeobox gene *goosecoid*. *Cell* **69**, 1097-1106.

Brook, F. A., Estibeiro, J. P. and Copp, A. J. (1991) Relationship between rate at embryonic develpoemnt and the preponderance of cranial neural tube defects in females. *Genet. Res.* **58**, 76.

Burgoyne, P. S. (1993). A Y-chromosomal effect on blastocyst cell number in mice. *Development* **117**, 341-345.

Champlin, A. K., Dorr, D. L. and Gates, A. H. (1973). Determining the stage of the estrous cycle in the mouse by the appearance of the vagina. *Biol. Reprod.* **8**, 491-494.

Cockroft, D. L. (1991). Dissection and culture of post-implantation mouse embryos. In *Postimplantation Mammalian Embryos: A Practical Approach*. (ed. A. J. Copp and D. L. Cockroft). Oxford: IRL Press.

Downs, K. M., Martin, G. M. and Bishop, J. M. (1989). Contrasting patterns of *myc* and N-*myc* expression during gastrulation of the mouse embryo. *Genes Dev.* **3**, 860-869.

Fujinaga, M. and Baden, J. M. (1992). Variation in development of rat embryos at the presomite period. *Teratology* **45**, 661-670.

Fujinaga, M., Brown, N. A. and Baden, J. M. (1992). Comparison of staging systems for the gastrulation and early neurulation period in rodents: a proposed new system. *Teratology* **46**, 183-190.

Goedbloed, J. F. (1972). The embryonic and postnatal growth of rat and mouse. *Acta anat.* **82**, 305-336.

Herrmann, B. G. (1991). Expression pattern of the *Brachyury* gene in whole-mount T^{Wis}/T^{Wis} mutant embryos. *Development* **113**, 913-917.

Hogan, B., Costantini, F. and Lacy, E. (1986). *Manipulating the Mouse Embryo. A Laboratory Manual. Section C.* New York: Cold Spring Harbor Laboratory.

Jurand, A. (1974). Some aspects of the development of the notochord in mouse embryos. *J. Embryol. Exp. Morph.* **32**, 1-33.

Kaufman, M. H. (1991). Morphological stages of postimplantation development. In *Postimplantation Mammalian Embryos: A Practical Approach*. (eds. A.J. Copp and D.L. Cockroft). Oxford: IRL Press.

Kaufman, M. H. (1992). *The Atlas of Mouse Development*. London: Academic Press.

Lawson, K. A. and Pedersen, R. A. (1987). Cell fate, morphogenetic movement and population kinetics of embryonic endoderm at the time of germ layer formation in the mouse. *Development* **101**, 627-652.

Lawson, K. A. and Pedersen, R. A. (1992). Early mesoderm formation in the mouse embryo. *Nato Advanced Study Workshop on Formation and Differentiation of Early Embryonic Mesoderm.* Banff, Canada. October 25-29, 1991. (eds. R. Bellairs and J.W. Lash). New York: Plenum Press, in press.

Lawson, K. A., Meneses, J. and Pedersen, R. A. (1991). Clonal analysis of epiblast fate during germ layer formation in the mouse embryo. *Development* **113**, 891-911.

Poelmann, R. E. (1981). The head process and the formation of the definitive endoderm in the mouse embryo. *Anat. Embryol.* **162**, 41-49.

Rugh, R. (1968). *The Mouse. Its Reproduction and Development.* Minneapolis: Burgess.

Seller, M. J. and Perkins-Cole, K. J. (1987). Sex difference in mouse embryonic development at neurulation. *J. Reprod. Fert.* **79**, 159-196.

Snell, G. B. and Stevens, L. C. (1966). Early Embryology. In *Biology of the Laboratory Mouse.* 2nd Edn. (ed. E. L. Green). New York: McGraw Hill.

Theiler, K. (1989). *The House Mouse. Development and Normal Stages from Fertilization to 4 Weeks of Age.* 2nd Edn. Berlin: Springer-Verlag.

Thornhill, A. R. and Burgoyne, P. S. (1993). A paternally imprinted X chromosome retards the development of the early mouse embryo. *Development*, in press.

Tsunoda, Y., Tokunaga, T. and Sugie, T. (1985). Altered sex ratio of live young after transfer of fast- and slow-developing mouse embryos. *Gamete Res.* **12**, 301-304.

Wilkinson, D. G., Bhatt, S. and Herrmann, B. G. (1990). Expression pattern of the mouse T gene and its role in mesoderm formation. *Nature* **343**, 657-659.

Yamaguchi, T. P., Conlon, R. A. and Rossant, J. (1992). Expression of the fibroblast growth factor receptor FGFR-1/flg during gastrulation and segmentation in the mouse embryo. *Dev. Biol.* **152**, 75-88.